Controlling Negative and Positive Power at the Ankle with a Soft Exosuit*

Sangjun Lee, *Student Member, IEEE*, Simona Crea, Philippe Malcolm, Ignacio Galiana, Alan Asbeck, and Conor Walsh, *Member, IEEE*

***Abstract* — The soft exosuit is a new approach for applying assistive forces over the wearer's body through load paths configured by the textile architecture. In this paper, we present a body-worn lower-extremity soft exosuit and a new control approach that can independently control the level of assistance that is provided during negative- and positive-power periods at the ankle. The exosuit was designed to create load paths assisting ankle plantarflexion and hip flexion, and the actuation system transmits forces from the motors to the suit via Bowden cables. A load cell and two gyro sensors per leg are used to measure real-time data, and the controller performs position control of the cable on a step-by-step basis with respect to the power delivered to the wearer's ankle by controlling two force parameters, the pretension and the active force. Human subjects testing results demonstrate that the controller is capable of modulating the amount of power delivered to the ankle joint. Also, significant reductions in metabolic rate (11%-15%) were observed, which indicates the potential of the proposed control approach to provide benefit to the wearer during walking.**

I. Introduction

Over the last decade, a number of lower-extremity exoskeletons have been developed to assist human gait in various conditions. Some devices have been designed to assist impaired [1, 2] or able-bodied [3-6] people, while others have been designed to make load carriage easier [7, 8]. Conventionally, these devices have consisted of rigid exoskeleton structures enabling high assistive torques to the wearer [9]. However, rigid frames can restrict the natural movement of the wearer and may apply undesired forces when they are misaligned with the wearer's biological joints [10]. Moreover, rigid devices may have large inertias particularly on distal areas, which can hinder the motion of the wearer [11] and provide challenges from a control perspective.

*This material is based upon the work supported by the Defense Advanced Research Projects Agency (DARPA), Warrior Web Program (Contract No. W911NF-14-C-0051). This work was also partially funded by the Wyss Institute for Biologically Inspired Engineering and the John A. Paulson School of Engineering and Applied Sciences at Harvard University.

S. Lee (e-mail: slee@seas.harvard.edu), P. Malcolm (e-mail: pmalcolm @seas.harvard.edu), I. Galiana (e-mail: ignacio.galianabujanda@wyss. harvard.edu) and C. Walsh (phone: 617-496-7128; e-mail: walsh@seas. harvard.edu) are with the John A. Paulson School of Engineering and Applied Sciences and the Wyss Institute for Biologically Inspired Engineering, Harvard University, MA 02138, USA.

S. Crea (e-mail: s.crea@sssup.it) is with the BioRobotics Institute, Scuola Superiore Sant'Anna, viale Rinaldo Piaggio, Pontedera (PI), Italy.

A. Asbeck (e-mail: aasbeck@vt.edu) is with the Department of Mechanical Engineering, Virginia Polytechnic Institute and State University, VA 24061, USA.

In an attempt to mitigate some of these challenges, devices composed of soft textiles, which are called soft exosuits, have been designed and studied [12-16]. The soft exosuits transmit tensile forces over the wearer's body through load paths determined by the textile architecture; thus, they are particularly suitable for assisting locomotion, e.g. walking, as they have extremely low distal inertia and create torques intrinsically aligned with the biological joints. These systems have several potential applications including helping soldiers or first responders to carry heavy loads with less energy and enabling impaired people to improve their mobility. While promising proof-of-concept results highlighting the benefits of soft exosuits have been shown, there remains much scope to explore how to control these devices given their inherent compliant and nonlinear mechanical structure.

Another open research question regarding gait assistive devices is the optimal assistance to the wearer, which maximizes the efficacy of the device; in particular, the best strategy for ankle assistance during the mid-stance phase (i.e. negative-power phase) is still uncertain. Some studies on ankle exoskeletons have presented that significant metabolic reductions are observed when majority of the assistance is given during the push-off, where the ankle joint power is positive [17]. More recently, however, a research group has reported that assisting both negative- and positive-power phases also results in significant reduction in metabolic cost [5]. These different results indicate that the underlying effects of negative-power assistance delivered to the ankle are still

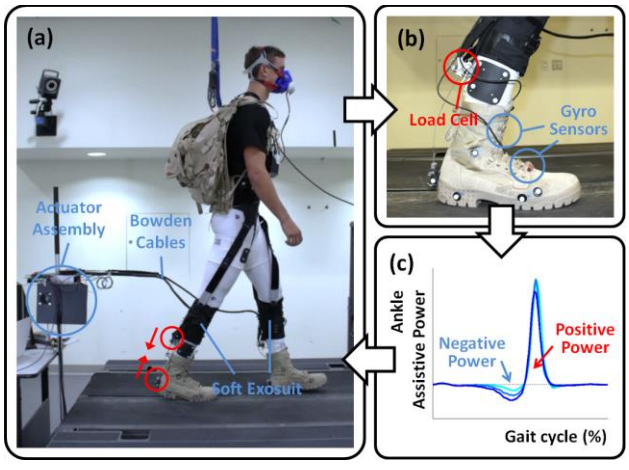

Figure 1 An overview of the study: (a) the soft exosuit (discussed in Section II), the actuation system (discussed in Section III), and the experimental setup (discussed in Section V), (b) sensors to measure the ankle speed and the force (discussed in Section III), and (c) ankle assistive power profiles with different negative power values (discussed in Section IV).

unclear.

In line with this, we present an updated version of the soft exosuit previously described in [14, 15] and a new control approach that can independently control the level of assistance that is provided during negative- and positive-power periods at the ankle joint. We then utilize this controller to perform a study where we (i) apply consistent assistance to the ankle during the push-off (i.e. positive-power phase), and at the same time, (ii) control the amount of the negative power absorption at the ankle within a gait cycle. While the majority of the assistance is delivered at push-off, this study allows us to investigate the effect of the negative-power assistance to the ankle, which may then provide an insight on the optimal assistance profile for the soft exosuit and other gait assistive devices. Here in this paper we describe the exosuit as well as the theory and implementation of the control approach. Additionally, we outline the experimental methods and include results showing the performance of the control strategy as well as metabolic expenditure of the wearer through human subjects testing.

II. Soft Exosuit

The soft exosuit used in this study is shown in Figure 2. It was designed by improving the exosuits for assisting ankle plantarflexion and hip flexion, which have been previously reported by our group [12-16, 18].

The suit for this study consists of a spandex base layer, a waist belt, a calf wrap on each leg, and two vertical straps per leg. The waist belt is similar to the one previously presented in [14, 15]. It wraps around the pelvis, which can bear relatively high forces compared to other parts of the body. It is secured with Velcro in the front, facilitating donning and doffing of the suit. The calf wrap fits tightly around the wearer's lower leg and helps to bear the load that is applied to the body. To fit the calf wrap to a range of body shapes and sizes, it was designed to consist of several Velcro tabs and a lace, and manufactured in four different sizes from XS to L. The leg straps connect the calf wrap to the waist belt and assist with distributing the actuation load between the calf and the waist to maximize the comfort. One end of the strap is attached to a buckle in front of the waist belt at the top of the thigh, while the other end is attached to a hook at the back of the calf wrap. The two leg straps for each leg were designed to respectively pass through medial and lateral sides of the knee joint. In addition, a metal bracket is attached to the wearer's boot, which bolts into the back of the heel.

Load paths configured by the suit textile architecture are similar to the multi-articular load path previously presented by our group [13]. In general, the load paths create forces on the body in parallel with the wearer's muscles; if forces are applied along the load path at the correct timing, it is expected that the wearer's muscles will adapt to the assistance, decreasing their activations and allowing the suit to do a portion of their work instead. In this study, the load paths were designed to apply assistive joint torques for ankle plantarflexion and hip flexion, simultaneously; more specifically, when the suit actuates the ankle joint, a portion of the total force is transmitted to the calf warp and the rest is transmitted to the waist belt via leg straps, creating a hip flexion torque (Figure 2). If a tension is created during the push-off phase of the gait cycle, activations of ankle plantarflexors, e.g. gastrocnemius and soleus, and hip flexors, e.g. rectus femoris and psoas, can be reduced, where both muscle groups present concentric contractions. For the knee joint, on the other hand, the suit load path was designed to pass approximately through the biological joint axis of the knee, particularly during the push-off, thus minimizing the effect of the tension in the suit at the knee joint.

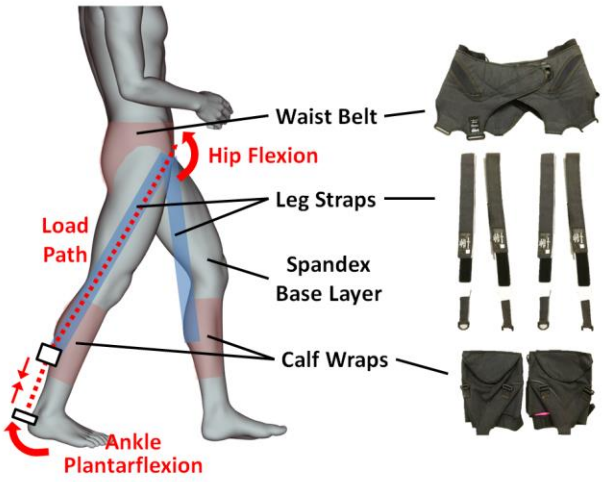

Figure 2 The soft exosuit used in this study. The right-hand-side figure shows the components of the suit, while the left figure shows the load path specified by the exosuit architecture.

III. Hardware Implementation

A. Actuation System

For the purposes of this study, we used an off-board actuation system shown in Figure 3(a), which is similar in principle to that described in [19, 20], but uses a different electromechanical design. The actuation system is composed of two Maxon EC-4 pole 30, 200W motors (part #305015, Maxon Motor Ag., Sachseln, Switzerland), and each motor connects to a 55:1 planetary gearbox which drives a 3-cm radius pulley.

Bowden cables are used to transmit the forces from the actuation system to the exosuit as shown in Figure 1(a). On the actuator side, the Bowden cable sheath connects to the outer frame of the pulley cover and its inner cable attaches to the pulley (Figure 3(a)). On the human side, the Bowden cable sheath connects to the back of the calf wrap, while its inner cable extends further to the metal bracket at the back of the heel (depicted as red circles in Figure 1(a)). When the motor rotates, the distance between the two points is shortened, generating forces not only at the ankle joint but also along the entire length of the exosuit multi-articular load path. This off-board actuation approach combined with the exosuit textile interface to the body enables forces to be delivered to the wearer with a very lightweight and flexible platform that is ideal for exploring human-machine interaction principles.

B. Sensors

As shown in Figure 1(b), a load cell and two gyro sensors per leg are used to measure real-time data of the wearer and the exosuit. The load cell (LTH300, Futek Advanced Sensor

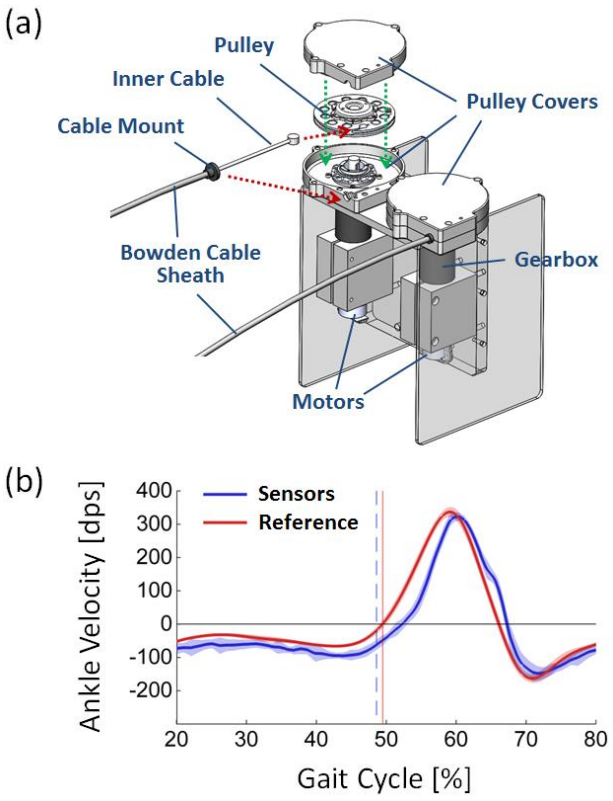

Figure 3 (a) A 3-D CAD model of the actuator system. (b) A representative comparison of the ankle joint speed measured by the sensors to the reference measured by motion capture. Solid lines indicate averaged profiles over 10 strides of a subject, while shaded areas indicate their standard deviations. Vertical lines near 50% of the gait cycle highlight the zero-crossing timings estimated by the two profiles, respectively (further discussed in Section IV).

Technology Inc., CA, USA) is located in series with the Bowden cable and the calf wrap to measure the force on the cable. In addition, two single-axis gyroscopes (LY3100ALH, ST Microelectronics, Geneva, Switzerland) are located on the boot: one at the top of the mid-foot and the other at the anterior side of the shank. Both gyro axes are aligned with the medio-lateral direction of the foot and the shank, respectively, to measure the sagittal angular speed of each segment.

Discussed further in Section IV, the signals from the two gyro sensors are used to calculate the ankle joint speed in real-time. Figure 3(b) shows a representative comparison between the ankle speed measured by the sensors and the reference measured by a commercial motion capture system (Vicon Motion Systems Ltd., Oxford, UK; 120 fps). The figure clearly demonstrates the ability of the gyro sensors to track the behavior of the ankle. From validation studies we conducted, we found the correlations between the two curves were higher than 92% across different subjects.

C. Control System Architecture

The electronics hardware for the system is based on Arduino Due, but modified and optimized for the exosuit. The control board integrates two servomotor drivers (Gold Twitter, Elmo Motion Control Ltd., NH, USA), two ARM-based processors (Cortex-M3, Atmel Corporation, CA, USA), electronics to read in signals from all of the sensors, and CAN for communication among all subsystems.

Each processor controls one actuator for each leg, performing the following tasks: (i) updating information from all of the sensors in the system over CAN, (ii) high-level control computations and the gait detection algorithm, (iii) communicating with low-level controllers (MC) over CAN to get motor information and to update control commands, (iv) sending data over serial communication to log system data, and (v) exchanging information with the other processor for the opposite leg so as to monitor overall system status.

IV. Control

A. Low-level Control Overview

To accomplish the goals of this study, we require a means to provide controlled forces to the wearer so as to control the level of positive power delivered to and negative power absorbed from the wearer. Given the compliance, friction and nonlinearity of the exosuit and cable-based transmission, we elect to perform position control of the motor, by monitoring the delivered force and iteratively adjusting the motor position to achieve the desired force in the exosuit. For this study, we define two different parameters that we wish to control, the pretension and the active force. In this section, using a simplified model, the rationale for these terms as well as the methodology for controlling them is discussed.

Simple position control model Figure 4(a) shows a schematic diagram of position control of the exosuit. Although the force on the cable (F_c) depends on many factors, a simplified model is considered here in this study to explain the concept how controlling the motor (and thus cable) position enables the force to be controlled.

First, assume that a person is wearing the suit while standing still without any joint motion. As the dynamics of the suit can be ignored, only the position change of the cable (x_c) can affect the force. As x_c increases, i.e. as the actuator pulls the cable further, F_c will also increase in reaction to the tensioning due to the effective human-suit stiffness that is a combination of the suit and the wearer's body as previously described in [18]; thus, F_c can be explained as an increasing function with respect to x_c.

$$F_c \sim f_{inc}(x_c)$$

Next, assume that the wearer is now in the "push-off posture" and is able to move the ankle joint only. This assumption is reasonable because the motion of the ankle is relatively greater and faster than the other parts of the body during the push-off. Similarly, F_c can be explained as an increasing function, but in this case, it is not just of x_c but of the relative motion between the cable and the ankle, i.e. $(x_c - x_a)$.

$$F_c \sim f'_{inc}(x_c - x_a)$$

As the displacement of the heel attachment (x_a) can be approximated as the product of the plantarflexion angle (θ_a) and the lever arm from the ankle joint center (d_a), F_c can be roughly expressed as follows.

$$F_c \sim f'_{inc}(x_c - \theta_a d_a)$$

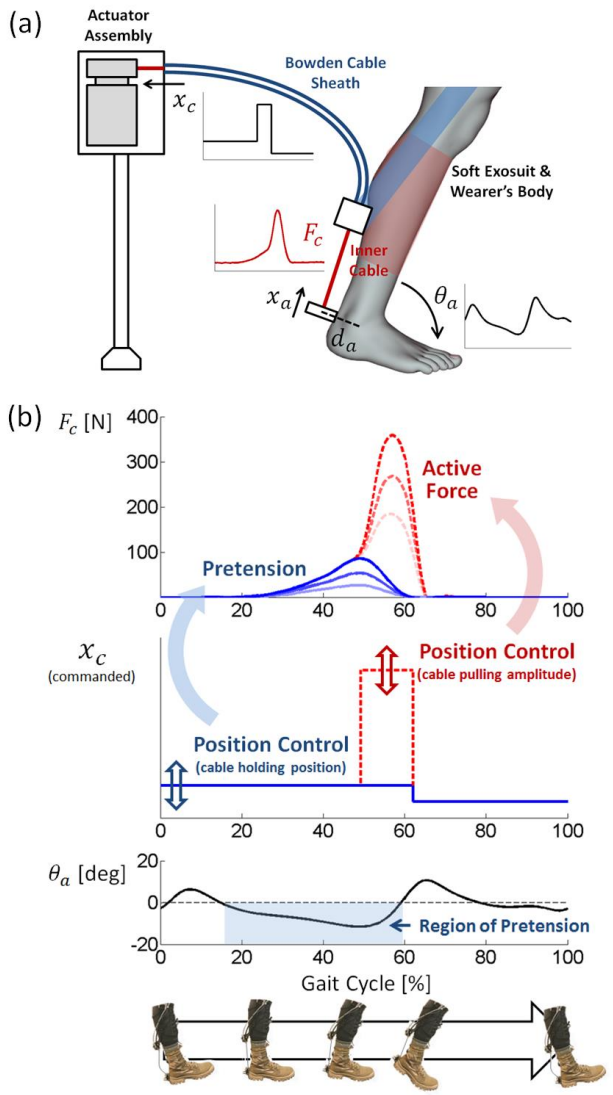

Figure 4 (a) A schematic diagram of position control model of the soft exosuit used in this study. (b) The methodology for controlling the pretension and the active force. The plots illustrate the force, the cable position (commanded), and the ankle plantarflexion angle within a gait cycle, respectively.

From this equation, the force generation can be classified into two, i.e. the pretension and the active force, with respect to the role of the cable position (x_c).

Pretension If the motor is just holding the cable in a position (x_c is a constant), F_c will be solely defined by θ_a. Thus, while walking with the suit, forces can be generated even without pulling the cable actively; this passive force is called pretension. As illustrated as blue curves in Figure 4(b), if x_c is kept constant while walking, the pretension is created when θ_a is negative, i.e. during the region of pretension, showing its maximum near 50% of the gait cycle when θ_a is minimized. In addition, the overall level of pretension can be controlled by adjusting the hold position of the cable, which makes x_c a bigger or a smaller constant in the above equation. (Note that, not to create undesired force or hinder the wearer's natural motion during the swing phase, x_c is decreased after 60% of the gait cycle by pushing the cable outward.)

Active force If higher forces are required during a given period of time, F_c can be enhanced by actively pulling the cable for the given phase, which will directly increase x_c; this is called active force. As depicted as red curves in Figure 4(b), the level of active force can also be controlled by adjusting the amplitude of x_c from its initial value for the given interval. (Note that, some amount of the active force remains even after x_c is decreased by pushing the cable out; this is because the force on the suit cannot decrease immediately due to the dynamics of the suit, which was ignored from the above equation so as to simplify the analysis.)

B. High-level Control Approach

In the proposed high-level control approach, the controller performs position control of the cable on a step-by-step basis with respect to the power delivered to the wearer's ankle. For this, the controller conducts a series of real-time computation, while the wearer is walking with the suit: (i) ankle speed zero-crossing detection, (ii) assistive power integration, and (iii) power-based position control. In this section, details about each step of these calculations and how it influences the high-level control is described.

Ankle speed zero-crossing detection As discussed in Section III, gyros are used to measure the ankle joint speed, and with this, we can estimate its zero-crossing that represents the transition from dorsiflexion to plantarflexion. Figure 5(a), (b), and (c) show typical patterns of the ankle joint kinematics and kinetics within a normal gait cycle. As shown in Figure 5(a), there are two distinct intervals where the biological ankle power is negative (30% to 50% of the gait cycle) and positive (50% to 70% of the gait cycle) during the stance phase [17]. As the joint power is the product of the joint speed and the joint moment, and also because the ankle joint moment is always positive (i.e. towards plantarflexion) during the mid- and the late-stance phases (Figure 5(b)), the transition from negative power to positive power corresponds to the zero-crossing of the ankle joint speed (Figure 5(c)).

Assistive power integration By using the timing of the zero-crossing, negative and positive power delivered within the current stride can be calculated. As the zero-crossing corresponds to the biological power transition from absorption to generation, the force applied before the zero-crossing will contribute only to the negative power; on the other hand, the force delivered after the zero-crossing will affect only the positive power at the ankle. In this study, the assistive power was calculated from the ankle speed and the force measured by the load cell, and then, it was integrated respectively within positive- and negative-power intervals and normalized by the stride time.

Power-based position control The controller then performs position control of the cable on a step-by-step basis using the two power integration values. To control the negative and the positive power respectively, the controller was designed to start pulling the cable right at the estimate of the zero-crossing of the ankle speed (Figure 5(d)). By doing so, the negative power for the next stride can be controlled by adjusting the level of pretension (as depicted in blue in Figure 5(d)), while the positive power can be changed by controlling the level of active force similarly to [6, 21, 22] (as depicted in red in Figure 5(d)). For example, if the negative power

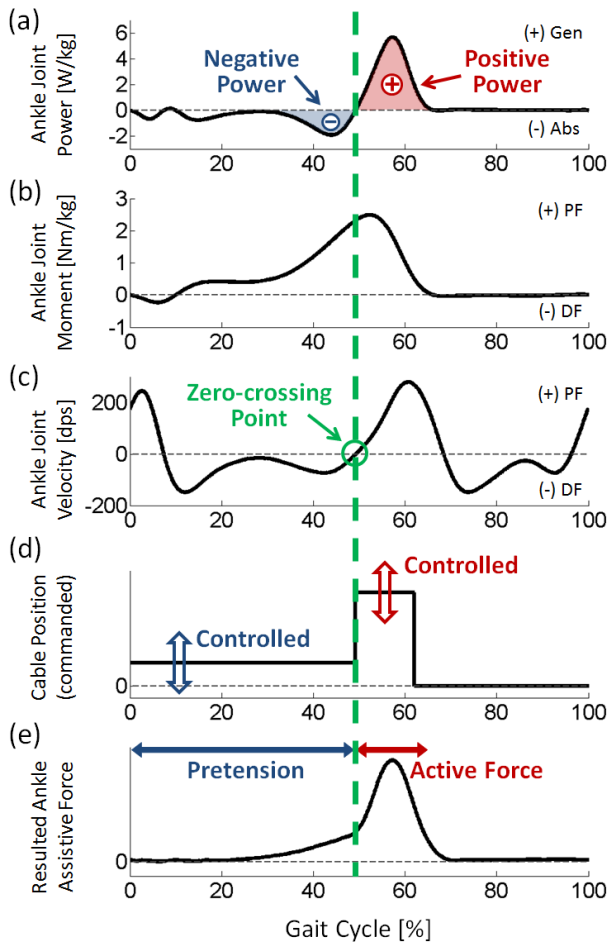

Figure 5 The rationale of the proposed high-level control approach. Typical kinematic and kinetic patterns of the ankle joint during a normal gait cycle: (a) joint power, (b) joint moment, and (c) joint speed. (d) A typical commanded cable position profile. (e) A typical ankle assistive force pattern resulted by the proposed control approach. (Gen: generation, Abs: absorption, PF: plantarflexion, DF: dorsiflexion)

integration during the current stride was less than the desired, the controller would increase the holding position of the cable to increase the pretension for the next stride; on the other hand, if the actual positive power for the current stride was greater than the desired value, the controller would reduce the amplitude of the cable position to decrease the active force for the next stride.

V. Human Walking Experiments

Human subjects testing, approved by the Harvard Medical School Institutional Review Board, was performed to evaluate the proposed control approach and its effect on metabolic expenditure of the wearer. Seven male subjects (26.3 ± 4.7 years; 79.9 ± 9.5 kg; 1.78 ± 0.06 m) with load-carrying experience participated in this study. To evaluate whether the controller was able to control the amount of negative power, the desired negative power was varied as 10%, 20%, and 30% of the positive power. The desired positive power kept as a constant which was subjectively selected during pilot testing, considering the maximum capability of the system to ensure that the system could achieve desired positive and negative power in all the experimental conditions. While wearing the soft exosuit, the participants walked on a treadmill at 1.5 m/s for 8 minutes per condition, carrying a 23-kg backpack (Figure 1(a)). The order of the conditions was randomized.

Figure 6(a) shows representative profiles of ankle assistive power segmented with the gait cycle, with the three different negative power values. As shown in the figure, the negative power to the ankle joint was clearly varied by the controller during the mid-stance phase (from 30% to 55% of the gait cycle) across the three different conditions, while the positive power kept constant during the push-off phase (from 55% to 70% of the gait cycle). Figure 6(b) highlights the performance of the controller more distinctly; the figure shows averaged positive power values (upward bars) and negative power values (downward bars) applied to the seven different subjects over the three different conditions, normalized by the desired positive power for each subject. As shown, different amount of negative power, i.e. 10%, 20%, and 30% of the positive power, were accurately delivered to all of the subjects, while the positive power was very close to 100% of the desired value for all subjects and conditions.

Figure 7 shows the peak pretension and the peak active force measured in the three conditions across the seven subjects. As shown in Figure 7(a), the peak of the pretension increased as the desired negative power increased. This indicates that, while the subject was walking with the suit, the controller properly increased the cable holding position to achieve the target negative power value, as desired. Interestingly, the peak active force also showed an increasing tendency with increasing negative power values, even though the positive power remained similar (Figure 7(b)). This may suggest that wearers tend to be adapted to the assistance to

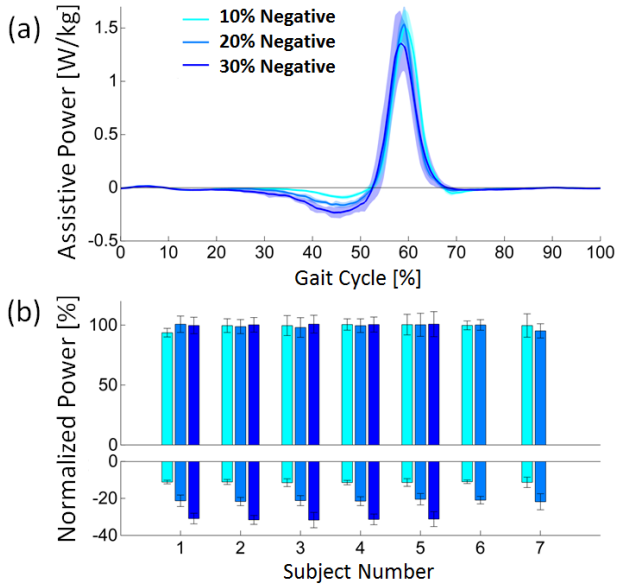

Figure 6 Assistive power applied to the wearer's ankle joint during the human subjects testing. (a) Representative profiles of power delivered within the gait cycle with different negative power values. Solid lines indicate averaged profiles over 10 strides of a subject, while shaded areas indicate their standard deviations. (b) Normalized positive powers (upward bars) and negative powers (downward bars) delivered to the seven subjects across the three conditions. Colored bars indicate averages, while error bars indicate their standard deviations. Note that two subjects could not finish the 30% condition due to technical issues.

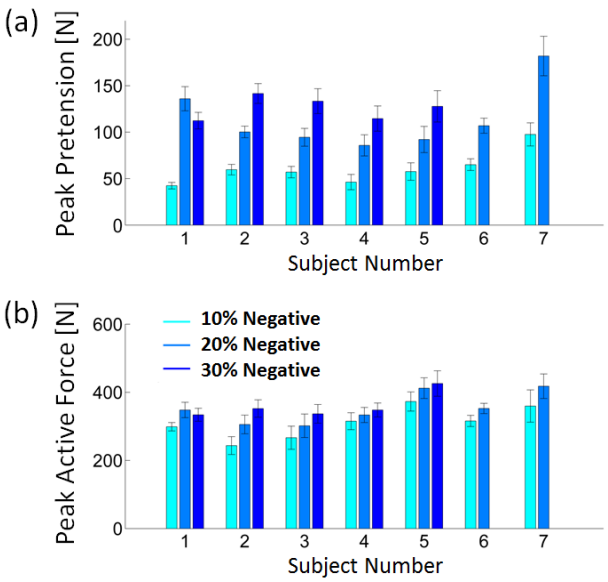

Figure 7 Force properties measured during the human subjects testing: (a) the peak pretension and (b) the peak active force measured in the three conditions across the seven subjects. Colored bars indicate averages, while error bars indicate their standard deviations.

have a higher peak active force when the pretension is already high at the beginning of the push-off, while getting the same amount of the positive-power assistance.

To assess the overall feasibility of the proposed controller and its effect on metabolic cost of the wearer, the O_2 consumption and the CO_2 production were measured (K4b2, COSMED, Rome, Italy) and the metabolic expenditure was calculated [23]. The three different controller conditions were compared to the fourth baseline condition, where the subject is walking with the load wearing the suit, but the actuators are turned off and the cables are slack, and thus, the suit applies minimal restrictions to the wearer beyond a very small level of added mass. Figure 8 illustrates averages and standard errors of metabolic reduction for the three conditions, compared to

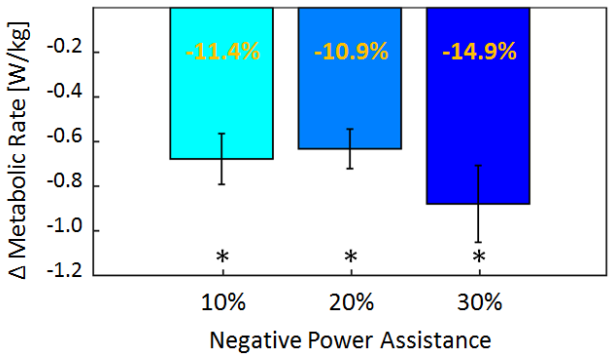

Figure 8 Changes in metabolic rates of the three conditions with different negative-power assistance, compared to the baseline condition. The net metabolic rates were 5.16 ± 0.15 W/kg, 5.22 ± 0.22 W/kg, and 5.00 ± 0.24 W/kg, respectively, while the baseline metabolic rate was 5.84 ± 0.20 W/kg (average ± SEM). Colored bars indicate averages, while error bars indicate their standard errors. Asterisks (*) indicate that all three conditions were significantly different from the baseline ($p < 0.007$), but no significant trend was found among them ($p = 0.25$).

the metabolic rates measured in baseline conditions averaged across the subjects. As can be seen, the metabolic cost of walking was significantly reduced for each of the three different conditions with values between 11% and 15% ($p < 0.007$, paired t-tests of the baseline versus other conditions with Sidak–Holm correction).

In the metabolic result, no significant trend was found with respect to the different negative-power assistance ($p = 0.25$, mixed-model ANOVA of metabolic reduction versus negative power assistance). This does not necessarily imply that the level of negative power to the ankle joint has no effect on the metabolic reduction. As already pointed out, some other parameters changed in addition to the negative power across conditions (e.g. peak active force), so in this study, the isolated effects of the negative power itself could not be precisely estimated.

VI. Conclusion

In conclusion, we have presented a body-worn lower-extremity soft exosuit and a new control approach that can independently control positive and negative power to the ankle. In human subjects testing, the controller was shown to be capable of modulating the amount of power delivered to the ankle joint, by controlling the pretension that determined the level of negative power absorption during dorsiflexion and the level of active force that determined the power delivered during plantarflexion. In addition, significant metabolic reductions (up to 14.9%) for each of the three actuation conditions indicated the potential of this control approach to provide benefit to a wearer during walking.

No significant trend was found with respect to the different negative-power assistance, but it should be noted that the result could be influenced by some other factors than the negative power absorption at the ankle. In general, it is challenging to control only a single parameter in such a human subject study due to the fact that many of the parameters are interrelated. For example, changes in negative power assistance may affect the overall way of walking even in other phases in the gait cycle. In addition, the current suit architecture also provides some amount of assistance for hip flexion, so the metabolic results presented may not be purely associated with the ankle joint. Therefore, further studies are needed to fully understand the effects of negative power delivered to the ankle.

Future work will include evaluating the performance of the exosuit and its controller in overgound studies as well as exploring the optimal control parameters across subjects and conditions, such as the optimal positive and negative power.

Acknowledgment

The authors would like to thank Fabricio Saucedo, Christopher Siviy, Adam Couture, Diana Wagner, Fausto Panizzolo and Kenneth G. Holt for their contribution to this work. S. L. also appreciates the financial support from the Samsung Scholarship.

REFERENCES

[1] J. Bae, S. M. M. De Rossi, K. O'Donnell, K. L. Hendron, L. N. Awad, T. R. T. Dos Santos, V. L. De Araujo, Y. Ding, K. G. Holt, T. D. Ellis, and C. J. Walsh, "A Soft Exosuit for Patients with Stroke: Feasibility Study with a Mobile Off-Board Actuation Unit," *in IEEE International Conference on Rehabilitation Robotics (ICORR)*, 2015.

[2] A. Esquenazi, M. Talaty, A. Packel, and M. Saulino, "The ReWalk Powered Exoskeleton to Restore Ambulatory Function to Individuals with Thoracic-Level Motor-Complete Spinal Cord Injury," *Am J Phys Med Rehabil*, vol. 91, 2012.

[3] P. Malcolm, W. Derave, S. Galle, and D. De Clercq, "A Simple Exoskeleton That Assists Plantarflexion Can Reduce the Metabolic Cost of Human Walking," *PLoS One*, vol. 8, 2013.

[4] L. M. Mooney, E. J. Rouse, and H. M. Herr, "Autonomous Exoskeleton Reduces Metabolic Cost of Human Walking," *J Neuroeng Rehabil*, vol. 11, 2014.

[5] S. H. Collins, M. B. Wiggin, and G. S. Sawicki, "Reducing the Energy Cost of Human Walking Using an Unpowered Exoskeleton," *Nature*, vol. 522, 2015.

[6] R. W. Jackson and S. H. Collins, "An Experimental Comparison of the Relative Benefits of Work and Torque Assistance in Ankle Exoskeletons," *J Appl Physiol*, Vol. 119, 2015.

[7] C. J. Walsh, D. Paluska, K. Pasch, W. Grand, A. Valiente, and H. Herr, "Development of a Lightweight, Underactuated Exoskeleton for Load-Carrying Augmentation," *in IEEE International Conference on Robotics and Automation (ICRA)*, 2006.

[8] L. M. Mooney, E. J. Rouse, and H. M. Herr, "Autonomous Exoskeleton Reduces Metabolic Cost of Human Walking During Load Carriage," *J Neuroeng Rehabil*, vol. 11, 2014.

[9] H. Herr, "Exoskeletons and Orthoses: Classification, Design Challenges and Future Directions," *J Neuroeng Rehabil*, vol. 6, 2009.

[10] S. Rossi, A. Colazza, M. Petrarca, E. Castelli, P. Cappa, and H. I. Krebs, "Feasibility Study of a Wearable Exoskeleton for Children: Is the Gait Altered by Adding Masses on Lower Limbs?," PLoS One, vol. 8, 2013.

[11] R. C. Browning, J. R. Modica, R. Kram, and A. Goswami, "The Effects of Adding Mass to the Legs on the Energetics and Biomechanics of Walking," *Med Sci Sport Exerc*, vol. 39, 2007.

[12] M. Wehner, B. Quinlivan, P. M. Aubin, E. Martinez-Villalpando, M. Baumann, L. Stirling, K. Holt, R. Wood, and C. Walsh, "A Lightweight Soft Exosuit for Gait Assistance," *in IEEE International Conference on Robotics and Automation (ICRA)*, 2013.

[13] A. T. Asbeck, R. J. Dyer, A. F. Larusson, and C. J. Walsh, "Biologically-Inspired Soft Exosuit," *in IEEE International Conference on Rehabilitation Robotics (ICORR)*, 2013.

[14] A. T. Asbeck, K. Schmidt, I. Galiana, D. Wagner, and C. J. Walsh, "Multi-Joint Soft Exosuit for Gait Assistance," *in IEEE International Conference on Robotics and Automation (ICRA)*, 2015.

[15] F. A. Panizzolo, I. Galiana, A. T. Asbeck, K. Schmidt, C. O'Neill, F. Saucedo, S. Allen, C. Siviy, P. Malcolm, K. G. Holt, and C. J. Walsh, "Evaluation of a Multi-Joint Soft Exosuit for Gait Assistance," *in International Symposium on Adaptive Motion of Animals and Machines (AMAM)*, 2015.

[16] A. T. Asbeck, K. Schmidt, and C. J. Walsh, "Soft Exosuit for Hip Assistance," *Rob Auton Syst*, vol. 73, 2015.

[17] D. A. Winter, "Energy Generation and Absorption at the Ankle and Knee During Fast, Natural, and Slow Cadences," *Clin Orthop Relat Res*, vol. 175, 1983.

[18] A. T. Asbeck, S. M. M. De Rossi, K. G. Holt, and C. J. Walsh, "A Biologically Inspired Soft Exosuit for Walking Assistance," *Int J Rob Res*, vol.34, 2015.

[19] Y. Ding, I. Galiana, A. Asbeck, B. Quinlivan, S. M. M. De Rossi, and C. Walsh, "Multi-Joint Actuation Platform for Lower Extremity Soft Exosuits" *in IEEE International Conference on Robotics and Automation (ICRA)*, 2014.

[20] Y. Ding, I. Galiana, A. T. Asbeck, S. M. M. De Rossi, J. Bae, T. R. T. Santos, V. L. Araujo, S. Lee, K. G. Holt, and C. Walsh, "Biomechanical and Physiological Evaluation of Multi-Joint Assistance with Soft Exosuits," *Trans Neural Syst Rehabil Eng*, 2016.

[21] P. Malcolm, R. E. Quesada, J. M. Caputo, and S. H. Collins, "The Influence of Push-Off Timing in a Robotic Ankle-Foot Prosthesis on the Energetics and Mechanics of Walking," *J Neuroeng Rehabil*, vol. 12, 2015.

[22] P. Malcolm, S. Galle, P. Van den Berghe, and D. De Clercq, "Analysis of Walking with Unilateral Exoskeleton Assistance Compared to Bilateral Assistance with Matched Work," *in Dynamic Walking Conference*, 2015.

[23] J. M. Brockway, "Derivation of Formulae Used to Calculate Energy Expenditure in Man," *Hum Nutr Clin Nutr*, vol. 41, 1987.